Texture of Crystalline Solids, 1980, Vol. 4, pp. 1-11
0309-7951/80/0401-0001$04.50/0

Printed in the United States of America

COMPARISON OF QUANTITATIVE TEXTURE ANALYSIS RESULTS FROM TIME-OF-FLIGHT AND CONVENTIONAL NEUTRON DIFFRACTION

K. FELDMANN, M. BETZL*, A. ANDREEFF, K. HENNIG*, K. KLEINSTÜCK**, and W. MATZ

Laboratory of Neutron Physics, Joint Institute for Nuclear Research, Dubna, USSR

**Central Institute for Nuclear Research Rossendorf, 8051 Dresden, P.O. Box 19, GDR*
***Technical University Dresden, 8027 Dresden, GDR*

(Received November 11, 1979)

Abstract: The adaptability of time-of-flight neutron diffraction for quantitative texture analysis is demonstrated. Measurements with this technique on drawn steel wire show good agreement with the results from conventional neutron diffraction experiments. A short description of the neutron time-of-flight method is given. Its application for texture investigations especially on low-symmetry crystalline systems, multiphase materials and for *in situ* studies is discussed.

INTRODUCTION

The aim of the present work is to show that neutron time-of-flight (TOF) diffraction (equivalent to energy dispersive X-ray diffraction) is a suitable tool for quantitative texture analysis. For this purpose the fibre texture of iron wire has been measured, first by conventional angle-dispersive neutron scattering and then using the time-of-flight technique. By comparing the quantitative results obtained by both methods the mathematical procedure for texture analysis by TOF diffraction is verified and some aspects of this method are discussed.

Texture investigations by means of the conventional angle-dispersive method using X-ray[1] as well as neutron diffraction[2] have been known for a long time. The series expansion technique proposed by Bunge[3] made it possible to describe the texture of materials quantitatively by calculating the so-called orientation distribution function using three parameters, e.g. the three Euler angles. Recently the

importance of energy-dispersive X-ray diffraction for texture investigations has increased, stimulated by efficient X-ray sources and synchrotron radiation.[4-6] A possibility of texture investigations using neutron time-of-flight technique was first shown by Szpunar et al.[7] in 1968 in a qualitative way. Up to now no publication is known concerning quantitative texture analysis by TOF neutron diffraction. In the present paper a transition to quantitative texture analysis using TOF technique is performed. This experiment is a part of the work on texture investigations by neutron time-of-flight diffraction planned for the new pulsed reactor IBR-2 of JINR Dubna.

EXPERIMENTAL METHODS

The conventional angle-dispersive neutron technique has been well known for some years. The diffractometer at the RFR reactor of CINR Rossendorf is described by Kleinstück et al.[2]

The TOF method uses the different velocities of neutrons with different energies and different wavelengths. If a pulsed polychromatic neutron beam from the reactor starts at time t_0, neutrons are incident on the sample at distance L_1 at different times depending on their velocities (Figure 1).

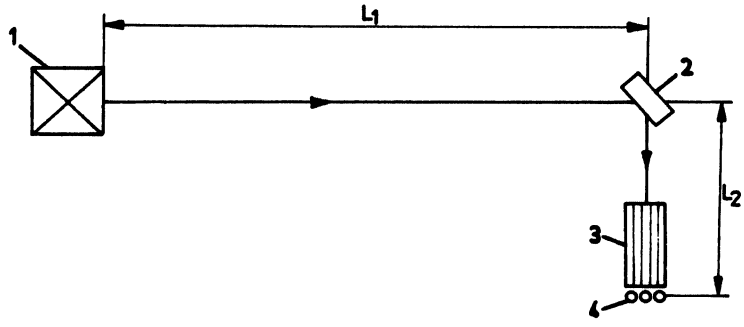

Figure 1. Schematic set-up of the TOF diffractometer at the pulsed reactor; L_1, the first flight path; L_2, the second flight path; 1, reactor; 2, specimen in the texture goniometer; 3, Soller collimator; 4, detector.

The time-of-flight spectrum of neutrons scattered according to Bragg's law

$$\lambda = 2d \sin \theta \qquad (1)$$

is measured by BF_3 counters connected with a multichannel time analyser. The relation between the time-of-flight $(t - t_0)$, energy E, mass m, and De Broglie wavelength, λ, of neutrons is given in Eq. (2),

$$t - t_0 = \frac{m\lambda}{h} (L_1 + L_2) = (L_1 + L_2) \sqrt{\frac{m}{2E}} \quad , \qquad (2)$$

where h is Planck's constant. The second flight path L_2 should be small, because the intensity decreases proportionally to $1/L_2^2$. The neutron time-of-flight diffraction is described in more detail by Buras and Holas.[8]

In the TOF method several Bragg reflections are recorded simultaneously. The information obtained at a fixed scattering angle and a fixed specimen orientation is sufficient for the determination of an inverse pole figure. Of course, the number of available Bragg reflections to construct inverse pole figure depends on spectrometer resolution. Alternatively, several normal pole figures can be measured with fixed scattering angle, varying the specimen orientation.

The neutron time-of-flight method is very suitable for studies on low-symmetry crystal systems, on multiphase materials and on axisymmetric samples. Furthermore, the TOF technique permits *in situ* investigations on specimens subjected to various controlled environments.

EXPERIMENTS

For all the investigations a steel wire of 3 mm diameter was used. Fastening several wires side by side in a special texture goniometer, a sample area of about 60 mm diameter was obtained. By suitable movement of the sample, the effective specimen volume in the beam was held constant. The intensities of one Bragg reflection were thus independent of absorption at various sample orientations.

The texture goniometer can be rotated independently about three perpendicular axes ψ, Ω, and ϕ. The smallest possible angular-step is 1 degree in each case. During the present investigation only the ψ-rotation was used (Figure 2).

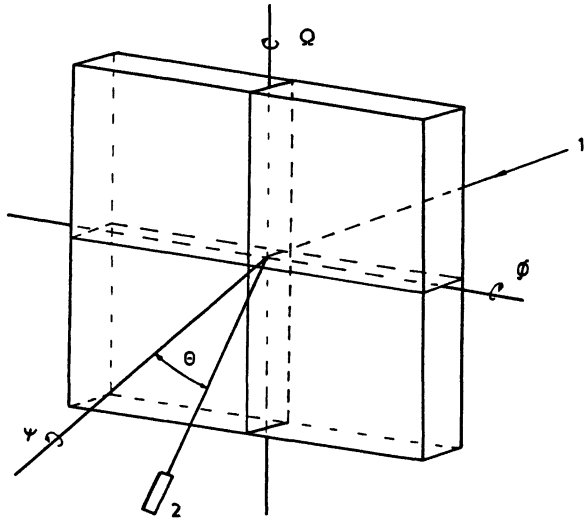

Figure 2. Schematic representation of the texture goniometer. Three independent axes for the transmission case are shown. (1, primary beam; 2, detector).

At the RFR reactor of CINR Rossendorf the pole figures {110}, {200}, {211} and {310} were measured in the range from the fibre axis to transverse direction in discrete angular steps of $\Delta\psi$ = 3 degrees. Pole figures are shown in Figure 3. The wavelength of the monochromatic beam was 1.058 Å.

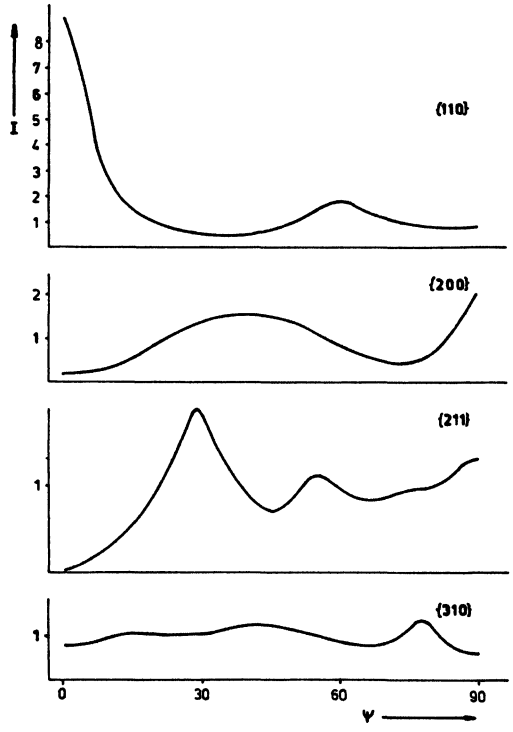

Figure 3. Normalized pole figures measured by the conventional method. Dependence of pole density I on specimen orientation ψ (in degrees) is given.

At the pulsed reactor IBR-30 of JINR Dubna the TOF diffraction spectra were measured on the same specimen. The sample orientation was varied in the range from the fibre axis to transverse direction in steps of $\Delta\psi$ = 6 degrees, i.e., normal pole figures were measured because only 8 reflections can be separated with the present spectrometer resolution.

In Figure 4 the TOF spectra for ψ = 0° (fibre axis), ψ = 30°, 60°, 90° are shown. The intensity variation of Bragg reflections from spectrum to spectrum is evident.

Parameters for the TOF experiment:

L_1 = 30.4 m
L_2 = 1.4 m
2ϑ = 90°
channel width 32 μs ($\Delta\lambda$ = 0.004 Å)
measuring time per one spectrum is 17,000 s.

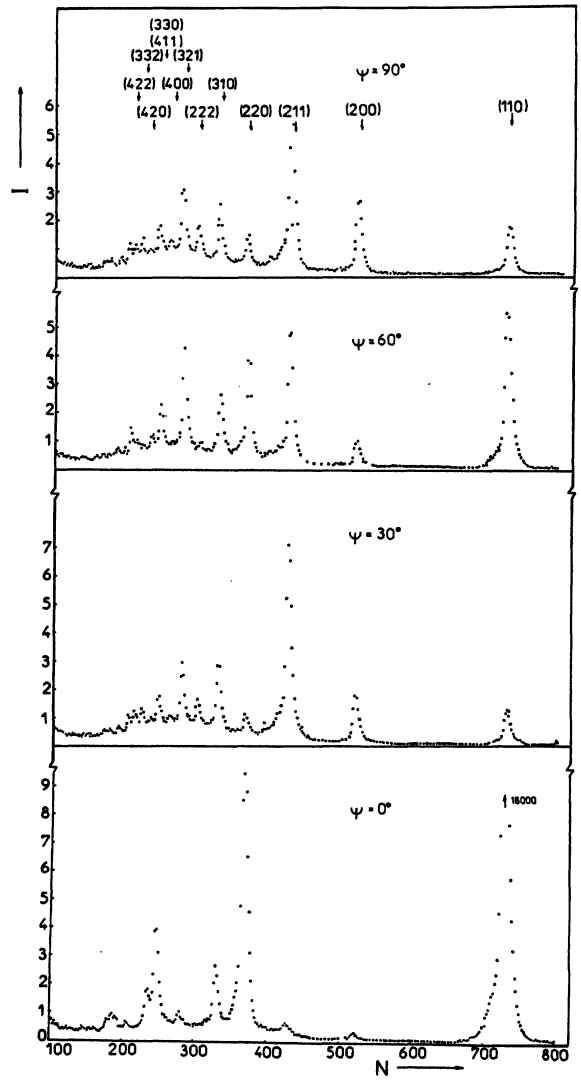

Figure 4. TOF diffraction spectra for different specimen orientations.

MATHEMATICAL TREATMENT

In the case of an axisymmetric specimen the inverse pole figure in the direction of the symmetry axis contains full information about the texture of investigated material. Unfortunately, the resolution of the spectrometer is too poor at present to determine inverse pole figure in a direct way. Therefore, the inverse pole figure of the symmetry axis has to be calculated from the normal pole figure data.

In the case of the conventional angle dispersive method the densities of unnormalized pole figures are measured directly. In TOF experiments the pole densities are proportional to the intensities of Bragg reflections. They have

been determined by means of a fit program taking into account the background, energy spectrum of the reactor pulse and asymmetric form of Bragg peaks. This form has been approximated by the asymmetric Lorentzian shape. It has also been possible using a fit program to separate the diffraction peaks which are partly overlapped. For the determination of pole figures the intensities of a fixed Bragg reflection must be compared for all specimen orientations. With variation of the sample orientation at a fixed scattering angle the position of the peak (hkℓ) does not change with respect to the wavelength (channel number of TOF spectrum). Therefore, all wavelength dependent quantities like Debye-Waller factor, absorption, extinction, etc., may not be taken into account. The normalization factors of each pole figure contain them. Further data handling process is the same for both methods. It is based on the well known series expansion method proposed by Bunge.[3] From the mathematical expansion for pole figures $\vec{h}_i = [hk\ell]$;

$$P_{\vec{h}_i}(\psi) = \sum_{l=0}^{\infty} F_\ell(h_i) P_\ell(\psi) \tag{3}$$

with

$$F_\ell(\vec{h}_i) = \sqrt{\frac{2}{2\ell + 1}} \sum_{\mu=1}^{M(\ell)} C_\ell^\mu \, k_\ell^\mu \, (\vec{h}_i) \tag{4}$$

$F_\ell(\vec{h}_i)$ coefficients can be calculated using orthonormality of Legendre polynomials $P_\ell(\psi)$

$$F_\ell(\vec{h}_i) = \frac{2}{N_{\vec{h}_i}} \int_0^{\pi} P_{\vec{h}_i}(\psi) \; P_\ell(\psi) \; \sin \psi \; d\psi \tag{5}$$

where ℓ is the power of series expansion, M(ℓ) is the number of linear independent spherical functions at power ℓ (see ref. 3, p. 32), $k_\ell^\mu(\vec{h}_i)$ are the spherical functions of the pole figure $\vec{h}_i$ containing all elements of crystal symmetry, C_ℓ^μ are the texture coefficients.

The normalization factor of pole figure $\vec{h}_i$ is calculated as follows:

$$N_{\vec{h}_i} = \int_0^{\pi} P_{\vec{h}_i}(\psi) \; \sin \psi \; d\psi \tag{6}$$

Usually the texture coefficients C_ℓ^μ are calculated by the least squares method.

$$\sum_i k_\ell^{\mu\,\prime} \left[F_\ell(\vec{h}_i) - \sqrt{\frac{2}{2\ell+1}} \sum_{\mu=1}^{M(\ell)} C_\ell^\mu \, k_\ell^\mu \, (\vec{h}_i) \right] = 0 \qquad (7)$$

Using thus determined coefficients the inverse pole figure of the symmetry axis $R_{sa}(\vec{h})$ can be calculated with an expression analogous to Eq. (3).

$$R_{sa}(\vec{h}) = \sum_{\ell=0}^{\infty} \sum_{\mu=1}^{M(\ell)} \sqrt{\frac{2}{2\ell+1}} \; C_\ell^\mu \, k_\ell^\mu \, (\vec{h}) \; P_\ell(0) \qquad (8)$$

At higher orders ℓ of series expansion the precision of integration [Eq. (5)] in dependence on the distance of measuring points in pole figures decreases rapidly with increasing number of oscillations of Legendre polynomials $P_\ell(\psi)$. Therefore, the density of points for integration has been increased with the help of quadratic interpolation. Of course, this procedure does not give any new information about the texture of the investigated material, but enables more complete use of information the pole figures contain.

DISCUSSION

A comparison of the pole figures measured by the conventional method and corresponding pole figures calculated from TOF spectra (Figure 5) shows good agreement. Moreover, four pole figures {222}, {321}, {420} and {332} could be separated in the TOF method.

From pole figure data measured by the conventional method the inverse pole figure of wire axis has been calculated by expanding the series up to $\ell = 34$. From comparing C_ℓ^μ-coefficients computed with and without interpolation, serious differences have been found suggesting an angular step of $\Delta\psi = 3°$ being sufficient for series expansion up to $\ell = 34$. The determined inverse pole figure is shown in Figure 6. In Figure 7 inverse pole figures are represented, which have been calculated from the TOF data taking into account different sets of pole figures. In all cases the series expansions were truncated at $\ell = 34$ also. The original data have been interpolated. The angular step was $\Delta\psi = 1°$ after that. The deviation of $F_2(\vec{h}_i)$ coefficients (see Table I) from zero was taken as a criterion for including or excluding the pole figures. This deviation may be used for characterizing the precision of pole figures.[3] As was expected all the inverse pole figures are similar. All calculated inverse pole figures are in good agreement with the literature.[1]

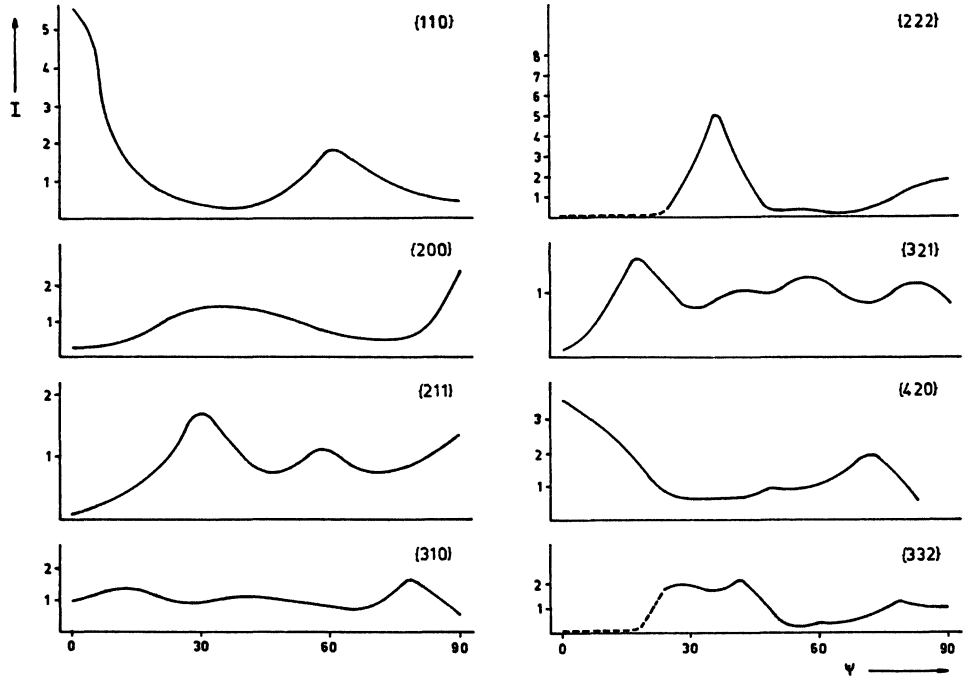

Figure 5. Normalized pole figures determined from the TOF spectra. Dependence of pole density I on specimen orientation ψ (in degrees). The dotted range of pole figures {222} and {332} is uncertain.

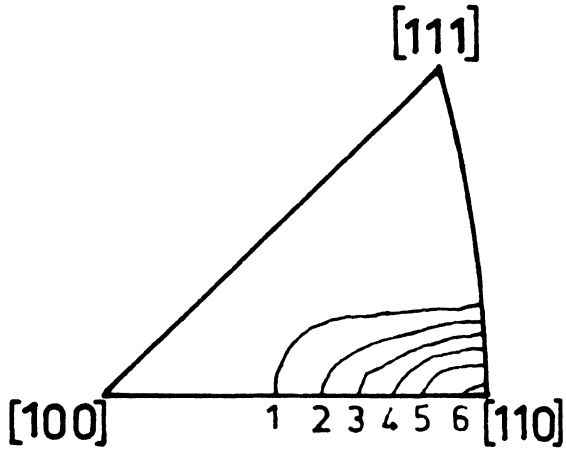

Figure 6. Inverse pole figure calculated from the conventional method data.

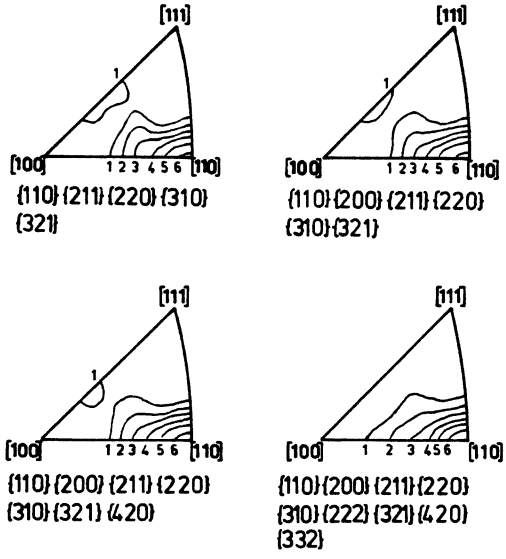

Figure 7. Inverse pole figures calculated from the TOF data taking into account different sets of pole figures. The pole figures used for the calculation are given.

TABLE I

$F_2(\vec{h}_i)$-Factors for Various Pole Figures

hkℓ	110	200	211	220	310	222	321	420	332
$F_2(\vec{h}_i)$	-0.025	0.155	0.042	0.024	-0.030	0.257	-0.022	0.039	0.338

In Table II, C_ℓ^μ-coefficients determined from the TOF data with and without interpolation are represented. The difference between the two sets is significant. The error is so large that the density maximum in the inverse pole figure is shifted from [110].

CONCLUSION

The present work is the first quantitative texture analysis by the neutron time-of-flight diffraction known to the authors. This method is shown to be a suitable tool for texture investigations. Because of a lot of simultaneously measurable Bragg reflections it appears to be very useful for nonstandard research, e.g. on low-symmetry crystalline systems, multiphase systems, etc. The method (good resolution is assumed) can be used efficiently for direct measurement of inverse pole figures, i.e. for *in situ* studies on a specimen subjected to any external influences. The high neutron flux

TABLE II

Texture Coefficients C_ℓ^μ, Determined from TOF Measurements Using Noninterpolated As Well As Interpolated Data. Pole Figures {110}, {200}, {211}, {220}, {310}, {321} and {420} Were Taken into Account

	Noninterpolated Data			Interpolated Data		
1	C_ℓ^1	C_ℓ^2	C_ℓ^3	C_ℓ^1	C_ℓ^2	C_ℓ^3
4	0.0567			0.0022		
6	-4.2443			-4.1534		
8	0.6016			0.5845		
10	-1.5126			-1.4024		
12	0.0484	-1.9934		-0.0960	-1.9302	
14	-0.5005			-0.5383		
16	-0.0941	-1.2424		0.0433	-0.9418	
18	-0.4962	0.8740		-0.2855	0.8322	
20	0.0366	-0.2882		-0.1065	-0.3934	
22	-0.0149	0.4930		-0.1200	0.2457	
24	1.1684	0.6778	-0.9386	0.5163	0.2846	-0.1819
26	-0.5990	-0.1456		-0.1741		
28	0.8727	1.1239	0.5831	0.2030	0.1684	0.1626
30	-0.5389	-0.8114	0.1069	-0.2278	-0.1128	0.0071
32	1.5229	-0.0523	-0.6723	0.1234	-0.0553	-0.0805
34	-0.6581	-1.2782	3.2690	-0.1020	-0.1926	-0.1126

of the IBR-2 reactor is expected to provide a significant progress in the neutron time-of-flight texture analysis.

ACKNOWLEDGEMENT

The authors are indebted to Dr. Yu. M. Ostanevich from JINR for valuable discussions and comments. M. B. expresses his gratitude to JINR for the stay during which the measurements were done.

REFERENCES

1. G. Wassermann and J. Grewen, *Texturen metallischer Werkstoffe* (Springer Verlag, Berlin-Göttingen-Heidelberg, 1962).
2. K. Kleinstück et al., *Kristall und Technik*, 11, 409 (1976).
3. H.-J. Bunge, *Mathematische Methoden der Texturanalyse*, (Akademie-Verlag, Berlin, 1969).
4. J. Szpunar et al., *Z. Metallk.*, 65, 221 (1974).
5. L. Gerward et al., *Texture*, 2, 95 (1976).
6. E. Laine et al., *Texture*, 2, 243 (1974).
7. J. Szpunar et al., *Nucleonica*, 13, 1111 (1968).
8. B. Buras and A. Holas, "Intensity and Resolution in the Time-of-Flight Powder Diffractometry," Report INR Nr. 745/II/PS, Warsaw, 1966.